

Quantum localization versus classical percolation and the metal-nonmetal transition in Hg-Xe films

K. Epstein,* A. M. Goldman, and A. M. Kadin

School of Physics and Astronomy, University of Minnesota, Minneapolis, Minnesota 55455

(Received 23 December 1982)

The electrical conductivities of films which are mixtures of Hg and Xe have been examined in the normal (nonsuperconducting) state as a function of composition. These films, which were quench condensed at $T=4.2$ K, were typically 5000 Å thick, and are believed to be microscopically homogeneous and fully three dimensional. Aspects of quantum theories of localization appear to more accurately describe the metal-nonmetal transition than classical percolation. Three distinct regimes of conductivity are evident: conventional transport for low Xe concentration, incipient localization, and strong localization with a negative temperature coefficient of resistance. Data in the second regime are compared with the scaling theory of localization, and a correlation length ξ is inferred. The transition to the insulating regime appears to be continuous, but a minimum metallic conductivity at $T=0$ K cannot be ruled out. The behavior of the superconducting transition with composition has also been examined within the context of localization theory.

I. INTRODUCTION

There has been considerable interest in recent years in elucidating the transition from metal to nonmetal in disordered materials.¹ Many experimental systems which exhibit such a transition consist of mixtures of metallic and insulating species.²⁻⁶ Two fundamentally different classes of theories have been used to explain the conductivity transition in these systems. In one approach, classical, geometrically based theories such as percolation⁷ have been applied to mixtures which are inhomogeneous on the macroscopic scale.⁶ However, their extended applicability to microscopically homogeneous mixtures⁸ is not generally accepted. In this latter regime, recent quantum theories of localization⁹⁻¹² have developed to a stage where comparison with experiments has shown promising agreement.^{4,5,13} In any given system, the relevance of microscopic or macroscopic models may depend on the degree of clustering of the components. Quantum localization is likely to be relevant if the length scales of the metallic clusters are smaller than the lengths associated with localization.

In one class of systems for observing the metal-nonmetal transition, films composed of a mixture of a good metal and a rare gas are prepared on substrates held at low temperatures, in order to freeze in the disorder.^{2,3} In the present study, we examine data on the conductivity of Hg-Xe alloys of various composition, alloys which we believe to be homo-

geneous down to a microscopic scale. A part of this data was previously analyzed within the context of "microscopic percolation."² The present study suggests that the metal-nonmetal transition in this system may be more completely explained using several aspects of the scaling theory of localization. Finally, since these samples tend to become superconducting at lower temperatures, we can correlate the development of the metal-nonmetal transition in the normal state with changes in the superconducting transition temperature.

In Sec. II of this paper several unique aspects of the apparatus and techniques used for sample preparation and electrical measurements are presented and the morphology of the films discussed. Section III is devoted to a presentation of the data and its analysis. The final section contains a discussion of superconductivity in this system and its relation to localization.

II. EXPERIMENTAL

The goal of the sample preparation technique was to prepare samples in a controlled manner which minimized the heating of the substrate during film growth. After preliminary evacuation of the internal chamber to a pressure of 10^{-8} Torr, a molecular-beam oven (a true Knudsen source) was heated to about 70°C, and allowed Hg and Xe vapor to intermix and thermalize before exiting through the orifice towards the substrate. The entire ap-

paratus was located inside a liquid-helium cryostat, so that the sample-holder assembly, including shutter and masks, could be maintained at a temperature of 4.2 K. The oven was surrounded, except for its orifice, by a liquid-nitrogen-cooled shroud, designed to attenuate greatly both the loss of liquid helium and the radiational heating of the sample. Furthermore, the condensation rate was kept sufficiently low (less than several Å/sec) that the film heating from the impinging atoms could be largely neglected. This in principle makes it possible for as-prepared films to be composed of an amorphous mixture of Hg and Xe atoms, rather than a mixture of macroscopic grains. Unfortunately, the evidence that the films are amorphous is rather indirect.^{3,14,15} We were unable to confirm it by structural analysis at room temperature, since as the films are heated up above about 10 K (still far too cold for the Xe atoms to sublime), they apparently begin to anneal or cluster in some way which irreversibly increases their conductivity. These latter films, with significantly different behavior,¹⁴ will not be discussed here. We are currently in the process of building an apparatus which will permit *in situ* low-temperature structure determination.

A number of samples of Hg-Xe alloys were fabricated, with compositions from pure Hg to 50 mol % Hg, and thicknesses ranging from 2000–10 000 Å. The compositions are nominal, in that they were calculated using oven parameters (oven temperature, Xe pressure, and geometrical factors). The calibration was, however, checked earlier with Na films that could be brought up to room temperature. The thickness is also estimated in that it is calculated using a packing fraction of $f=0.60$, which is appropriate for random close packing of similar-sized spheres.¹⁶ We have also used a hard-sphere model to estimate the volume fraction of mercury (VFM) V_f , using the formula

$$V_f = f(Xr_{\text{Hg}}^3)/(Xr_{\text{Hg}}^3 + (1-X)r_{\text{Xe}}^3), \quad (1)$$

where X is the molar fraction of mercury (MFM) and atomic radii $r_{\text{Hg}}=1.49$ Å and $r_{\text{Xe}}=2.16$ Å were used.³ Over the range of composition studied, V_f varied from about 0.60 (pure Hg) to about 0.15 VFM.

III. DATA AND ANALYSIS

A key feature of previous studies of the metal-nonmetal transition in metal-gas systems has been the presentation of data on the conductivity in a logarithmic plot of the conductivity σ as a function of composition. Figure 1 is just such a plot at low temperatures ($T=5$ K). Its range is such as to include all 6 orders of magnitude of the variation of the con-

ductivity with composition. The sample resistivities varied from a clearly metallic $20 \mu\Omega \text{ cm}$ to a clearly insulating $30 \Omega \text{ cm}$. The conductivity begins to fall dramatically at a molar concentration of about 60% Hg, which we will later identify more convincingly as the location of the metal-insulator transition. We will show below that a single plot of this type, which seems to suggest the applicability of percolation, obscures some of the more subtle details of the behavior near the metal-insulator transition, which become more evident when plotted on a linear scale over a more restricted range.

The composition dependence of the superconducting critical temperature T_{c0} is also shown in Fig. 1. A more complete discussion of this will be carried out later, but for the present it is sufficient to note that most of the samples became superconducting below about 4 K. It is for this reason that the normal-state conductivities were measured only at 5 K or above, so as to exclude the effects of superconducting fluctuations. Also, the samples began to anneal if heated above about 10 K, so that it was not possible to measure resistivity over a wide-enough temperature range to allow extrapolations to $T=0$.

We were able, however, to measure the temperature coefficient of resistivity (TCR), $(1/\rho)d\rho/dT$, over the range from 5 to 8 K, and this data is also plotted as a function of composition in Fig. 1. It goes from slightly positive on the metallic side to sharply negative on the insulating side, with the most dramatic change occurring, again, at around 0.60 MFM. It should be noted that the resistivity at which the TCR changes sign is the same as that reported in the work on Hg (Xe) done in Tel Aviv.³ The composition at which this transition occurs appears to differ in the two cases, however, perhaps as a consequence of a systematic difference in the composition calibrations or of a difference in the packing of the films, which were made using somewhat different processes.

If our assumption of a random dispersion of individual Xe atoms is correct, one expects that the regime of low Xe concentration should correspond to "linear dilution," that the additional resistance should be proportional to the concentration of Xe atoms. In terms of the scattering cross section Σ , the resistivity can be expressed as

$$\begin{aligned} \rho &= \hbar k_F / ne^2 l \\ &\simeq 3\hbar / [n^{2/3} e^2 (n_{\text{Xe}} \Sigma + 1/l_{\text{Hg}})], \end{aligned} \quad (2)$$

where n is the density of conduction electrons, $n_{\text{Xe}}=(1-X)n_{\text{Hg}}$ is the density of Xe atoms, l is the total electronic mean free path, l_{Hg} is the intrinsic mean free path in a pure Hg film, and $k_F=(3\pi^2 n)^{1/3}$ is the Fermi wave vector. (We are

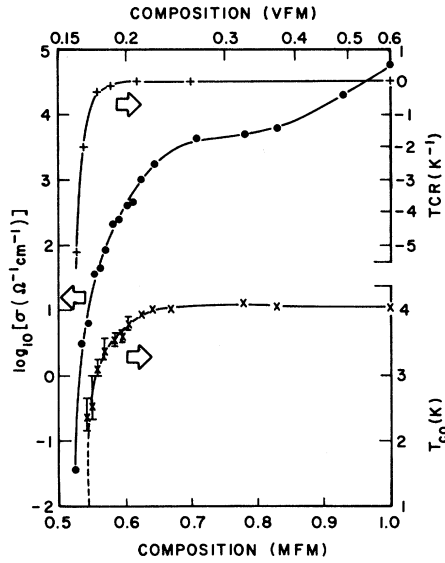


FIG. 1. Composition dependence of the normal-state and superconducting properties of Hg-Xe alloys. The conductivity σ at $T=5$ K (in $\Omega^{-1}\text{cm}^{-1}$, symbolized by closed circles) is plotted on a log scale vs the composition measured in mole-fraction mercury (MFM), from insulating samples on the left to pure mercury at the right. Some of the data points actually represent averages of several samples. The composition in terms of volume-fraction Hg (VFM) is indicated on the upper border. Also plotted are the temperature coefficient of resistivity [TCR= $d(\ln\rho)/dT$], indicated by +] measured over the range from 5 to 8 K, and the superconducting critical temperature T_{c0} (in K, indicated by x), defined by the halfpoint in the resistive transition [$R(T_{c0})=R_N/2$]. The "error bars" on some of the data for T_{c0} represents the width of the resistive transition from $T(0.9R_N)$ to $T(0.1R_N)$; those without these bars show an overall transition width of less than 50 mK. The dashed line represents an apparent jump to $T_{c0}=0$ at a composition of 17 VFM=54 MFM. The solid lines are a guide to the eye.

taking a free electron picture for simplicity.) In Fig. 2 we have plotted resistivity ρ versus the mole fraction, X , of Hg, and the straight-line fit for $X > 0.7$ (less than 25% Xe by volume) suggests that this approach may be valid. If the packing fraction is 0.6, and we take two conduction electrons per Hg atom, we can express the slope of this straight line as $d\rho/dX=(2.8 \times 10^{11} \Omega/\text{cm})\Sigma(\text{cm}^2)=8.3 \times 10^{-4} \Omega\text{cm}$. The resulting inferred cross section $\Sigma=(5 \text{ \AA})^2$ is quite reasonable in view of the approximations made here, and appears to support our contention of an amorphous random mixture.

This conventional picture should break down as

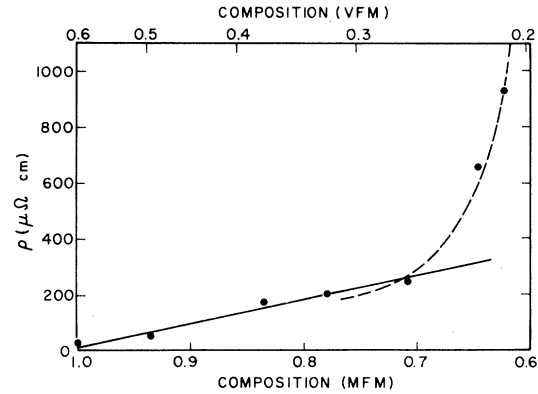


FIG. 2. Resistivity ($\mu\Omega\text{cm}$) vs composition (in MFM). The solid line is a fit to the "linear-dilution" model [Eq. (2)], corresponding to a scattering cross section per Xe atom of $\Sigma=25 \text{ \AA}^2$. The dashed line is an aid to the eye.

$k_F l \rightarrow 1$ (the Ioffe-Regel condition¹), or, equivalently, when l is approximately the interatomic spacing a . At this point, $\rho=O(1)\hbar a/e^2$, and in the present case, if we take $a=4 \text{ \AA}$, the regime close to $200 \mu\Omega\text{cm}$ seems to fit both descriptions, and to begin the deviation from the conventional transport behavior in Fig. 2 as well.

In Fig. 3 we have plotted the conductivity on a linear scale as a function of the composition in

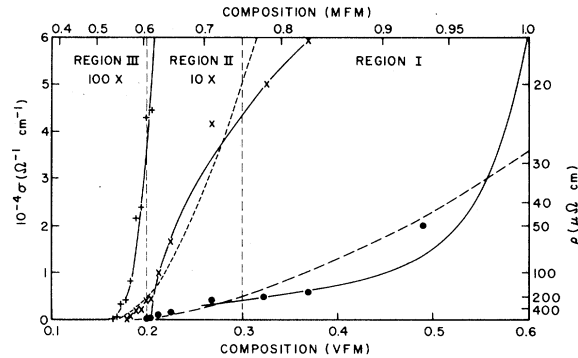


FIG. 3. Conductivity ($\Omega^{-1}\text{cm}^{-1}$) on a linear scale vs composition in VFM. The points labeled with closed circles are scaled as indicated on the axes, and the solid line in region I comes from the fit of Fig. 2. The points labeled with x , mostly in region II, are expanded vertically by a factor of 10, and the solid line through them is a fit to Eq. (4) with $n_c=0.203$ VFM, $\nu=0.6$, and $B=1.1$. The points in region III, indicated by +, are blown up by an additional factor of 10, and the line through them is merely a visual guide. Note in particular the two changes in concavity through the regions. The dashed curves are an attempted fit to percolation theory with Eq. (6), as discussed in the text, for all the data in regions I and II, with a single "critical exponent" $\nu=1.6$.

VFM (proportional to the concentration of conduction electrons). The vertical scale is expanded by two consecutive factors of 10 to show more clearly the lower conductivity data. The regime of conventional transport discussed earlier is now on the right (region I). There are two other regimes, as indicated by the change from concave upward to concave downward, and back to concave upward.

In the range between 0.2 and 0.3 VFM, conventional transport clearly does not apply, but the material also does not seem to be an insulator, since the TCR is zero or very slightly positive (cf. Fig. 1). We suggest that this range may be associated with the regime of incipient localization, as has been developed in scaling theory of localization.^{9,10} In this regime, even though the electronic states are still extended, they exhibit local variations of density over a scale up to the localization correlation length ξ , which is greater than the lattice size a . As the electronic density is decreased, ξ is expected to increase, diverging at the actual metal-insulator transition (at $T=0$) with a characteristic exponent $\nu \approx 1$ according to the formula

$$\xi = a[(n - n_c)/n_c]^{-\nu}. \quad (3)$$

In this regime, the resistivity is expected to scale with ξ , so that

$$\begin{aligned} \sigma(n) &= Be^2/\hbar\xi \\ &= (Be^2/\hbar a)[(n - n_c)/n_c]^\nu. \end{aligned} \quad (4)$$

We can obtain a reasonable fit to this expression, with a set of parameters that depends somewhat on the range of concentration we include. For instance, if we fit over the entire convex regime from 0.205 to 0.32 VFM, the best fit occurs for $n_c = 0.203$ VFM, $\nu = 0.6$, and $B = 1.1$ (taking again $a = 4$ Å). If the fit is restricted to the range 0.205–0.27 VFM, then $n_c = 0.198$ VFM, $\nu = 0.97$, and $B = 2$. By way of comparison, an exponent $\nu = 0.55$ was measured in the conductance of crystals of P-doped Si (Si:P) in the comparable regime.¹³

Since the data here are taken at finite temperature, the conductivity should not go all the way to zero at the metal-insulator transition. According to the scaling theory of localization, when the diverging ξ becomes larger than the inelastic diffusion length $l_i = (D\tau_i)^{1/2}$, where D is the electronic diffusion constant and τ_i the inelastic collision time, l_i should be substituted for ξ in Eq. (4) for the conductivity. This would appear to be the case near 0.20 VFM, where $\sigma = 400$ ($\Omega \text{ cm}$)⁻¹, which corresponds to a value of l_i of order 100 Å. This may seem a bit small, but for comparison a value of 250 Å was inferred in a localization study on a W-Re alloy.¹⁷

An alternative explanation of this incipient localiza-

tion regime has been provided by Mott and Kaveh.¹¹ In this approach, there is a sharp, well-defined minimum metallic conductivity at $T=0$, with a value

$$\sigma_{\min} \approx 0.03e^2/\hbar a \approx 200 \Omega^{-1} \text{ cm}^{-1}.$$

This value seems to be at about the bottom of the range of conductance within the incipient localization regime. For lower conductances, the TCR is negative. There is no need to invoke a value of l_{in} to act as a cutoff for a correlation length. We cannot at present rule out the possibility that $\sigma = 200\text{--}300 \Omega^{-1} \text{ cm}^{-1}$ represents the minimum metallic conductivity, given the limited temperature range over which these samples can be varied. Furthermore, Kaveh and Mott¹¹ have proposed a formula for the conductivity in the “incipient localization” regime

$$\sigma = \sigma_B [1 - 3/(k_F l)^2], \quad (5)$$

where σ_B is the form in the regime of conventional transport [Eq. (2)]. This should begin to deviate from σ_B for $\sigma \approx 0.2e^2/\hbar a \approx 3000 \Omega^{-1} \text{ cm}^{-1}$, and should approximately fit a power law $\sigma \sim (n - n_c)^\nu$, where ν changes from about 0.6 away from the transition to 2 as $n \rightarrow n_c$. This, too, is reasonably consistent with the data for these Hg-Xe films, as well as the earlier data on Si:P that it was proposed to explain.¹³

Finally, for concentrations lower than 0.20 VFM, the TCR starts to turn sharply negative, suggesting a strongly localized intrinsically insulating state, with conduction occurring by some sort of thermal activation process. Several possibilities have been suggested theoretically for conduction in a localized regime. Imry¹⁰ has proposed a phonon-assisted diffusion between localized states with $\sigma = (\xi^2/\tau_i)e^2 N(0)$, where τ_i is the inelastic scattering time, ξ is here the size of the localized states, which diverges at the transition, and $N(0)$ is the density of states at the Fermi surface. Alternatively, Mott¹ has suggested variable-range hopping (VRH) where $\ln \rho \sim T^{-1/4}$, which has in fact been reported in a number of insulating systems. For the as-prepared Hg-Xe films, the range of accessible temperatures was rather limited, preventing an accurate determination of the mechanism of conduction. Samples which had been annealed to 20 K, however, maintained their structure upon being cooled down, and in some of these samples, with concentration less than 0.17 VFM, the characteristic temperature dependence of VRH was obtained. It is not known whether this is also applicable to the as-prepared films.

In an earlier publication, we had proposed “microscopic percolation” as a way to fit the conductivity data. The form predicted from percolation

theory, at least sufficiently close to the critical volume fraction n_c , is

$$\sigma = \sigma_0 [(n - n_c)/n_c]^\nu. \quad (6)$$

One could conceivably fit to the entire range of data, including these points where the TCR is negative. If that is done, a best fit yields $n_c = 0.16$ VFM and $\nu = 2.2$, with a rather large standard deviation. Somewhat more reasonably, the points for $n < 0.20$ VFM can be removed from the fit, since percolation should ostensibly describe conduction between metallic clusters via metallic links. If this is done, a best fit gives $n_c = 0.17$ VFM and $\nu = 1.6$, with a somewhat smaller error. Since the values of both n_c and ν from this fit are in reasonable accord with theoretical predictions of classical percolation in three dimensions,⁷ it was thought earlier that some sort of microscopic percolation might in fact be appropriate to this system. However, when we plot this fit together with the data in Fig. 3, it becomes clear that the agreement with percolation theory is largely an artifact of the points included in the fit. In particular, percolation with a single exponent cannot explain the change in concavity, nor can it account for the coincidence of the inflection point near the Ioffe-Regel conductivity. Furthermore, if we remove the two most mercury-rich points from the fit, the optimum values are changed to $n_c = 0.195$ and $\nu = 0.83$, with a substantially reduced error. This, taken together with the questionable applicability of percolation to this system and the more reasonable agreement with localization, suggests that percolation is unlikely to be the explanation for the metal-insulator transition in these samples.

IV. SUPERCONDUCTIVITY AND DISCUSSION

As we noted earlier, Fig. 1 includes a plot of the superconducting critical temperature T_{c0} of these films as a function of composition, where T_{c0} is defined by $\rho(T_{c0}) = 0.5\rho_N$. Clearly, the critical temperature is largely unaffected by the increasing disorder through the conventional transport regime, and starts to decrease in the regime of incipient localization. This result is consistent with Anderson's theorem,¹⁸ which states that pair breaking in singlet-paired superconductors cannot take place as a result of scattering from nonmagnetic impurities. This is in sharp contrast to certain other materials, in particular granular aluminum,⁵ for which the critical temperature initially rises dramatically as the normal-state resistivity is increased. However, Anderson's theorem would not be expected to hold when the electronic wave functions become spatially

localized, and in fact the values of T_{c0} for Hg-Xe dropped sharply as the TCR in the normal state became more negative. The transition itself also broadened somewhat as the resistivity was increased, but it was not until the strongly localized samples that it began to be very wide (see the "error bars" in Fig. 1). No samples with $T_{c0} < 2$ K were measured, suggesting a very sharp or even discontinuous change for concentrations less than 0.17 VFM.

We believe that the samples reported here are likely to be three dimensional in the contexts of both electronic localization and superconductivity, since the film thicknesses are much greater than either the inelastic diffusion length l_i or the superconducting coherence length. We have elsewhere¹⁹ examined much thinner films of Hg-Xe (typically 100–200 Å in thickness) near the metal-insulator transition, which followed the two-dimensional theory of the superconducting transition, including the dependence on the sheet resistance $R_N^\square = \rho_N/d$. In contrast, the critical temperatures of the films in this work correlate not with R_N^\square , but rather with the resistivity ρ_N , as the thickness is varied, suggesting that they are properly three dimensional.

A complete theoretical analysis of the interaction between superconductivity and localization has thus far been given only for the two-dimensional case.²⁰ Nevertheless, a preliminary, qualitative analysis can be presented based on suggestions by Imry and Strongin²¹ and McMillian.²² For an amorphous metal, or one with sufficiently small grains, superconductivity should disappear at the same point as does normal metallic conduction, due in part to the decrease in the electronic density of states $N(0)$ at the Fermi energy. We continue to see superconductivity for samples which appear to be localized, i.e., with a negative TCR in the normal state. This suggests that at finite temperatures, inelastic scattering may act to maintain an extended superconducting state, in much the same way as l_{in} acts to cut off the divergence in ξ in the scaling theory. A possible consequence might be that at lower temperatures, when l_{in} is longer, some of these superconducting samples may reenter the normal state, becoming insulators at $T = 0$. We saw no direct evidence of this, in part because the samples could not be cooled below about 1.4 K, and this is a subject of continuing investigation.

If we consider the behavior of $N(0)$ near the metal-insulator transition quantitatively and its effect on the superconducting T_c , one has approximately, after McMillian,^{12,22}

$$\ln T_c \sim 1/N(0) \sim (\xi/a)^{3-\eta} \sim (n - n_c)^{3-\eta}. \quad (7)$$

If we fit to the data for concentrations greater than 0.20 VFM (although as noted above these are not

$T=0$ measurements), we obtain $3-\eta=0.02$, or $\eta=2.98$. This reflects only the weak dependence of T_c on the composition on the metallic side, and is unlikely to be definitive. Clearly, more work in this area is needed.

To summarize, we have examined the conductivities of a series of three-dimensional quench-condensed Hg-Xe alloys, which we believe to be microscopically homogeneous, as a function of the composition. By plotting the conductance on a linear, rather than a logarithmic scale, we see three different regimes. In the first, conventional transport, we can interpret the increase in resistivity as being due to scattering off single Xe atoms. As the concentration of Xe is increased, and the Ioffe-Regel resistivity passed, we see evidence of incipient localization, and can fit to a diverging localization correlating length, as predicted according to the scaling theory of localization. An alternative formulation which includes a minimum metallic conductivity cannot, however, be ruled out. The transition to a strongly localized state, with a negative TCR, occurs at about 0.20 VFM, 0.60 by mole fraction mercury. The mechanism of conduction in this regime is un-

clear, due to the limited range of temperature possible. In an earlier paper, some of the same data from at least two of the three ranges were fitted to a single power law, in an attempt to compare to percolation theory. On a linear scale, the earlier agreement does not look quite as good. Finally, the superconducting critical temperature is only weakly dependent on composition until the metal-insulator transition is approached, making this system a good one to test theories of the interaction of localization and superconductivity. Further work in these areas is continuing.

ACKNOWLEDGMENTS

The authors would like to thank E. D. Dahlberg for useful discussions and for assistance with earlier stages of the present work. This work has been supported in part by the National Science Foundation under Grants Nos. NSF/DMR-80-11948, NSF/DMR-80-06959, and NSF/DMR-80-15310 and by the Graduate School of the University of Minnesota.

*Present address: 3M Technical Labs, St. Paul, Minnesota 55144.

¹N. F. Mott, *Metal-Insulator Transitions* (Taylor and Francis, London, 1974).

²K. Epstein, E. D. Dahlberg, and A. M. Goldman, *Phys. Rev. Lett.* **43**, 1889 (1979).

³O. Cheshnovski, U. Even, and J. Jortner, *Solid State Commun.* **22**, 745 (1977); *Philos. Mag.* **B 44**, 1 (1981); *Phys. Rev. B* **25**, 3350 (1982).

⁴B. W. Dodson, W. L. McMillan, J. M. Mochel, and R. C. Dynes, *Phys. Rev. Lett.* **46**, 46 (1981).

⁵R. C. Dynes and J. P. Garno, *Phys. Rev. Lett.* **46**, 137 (1981).

⁶G. Deutscher and M. Rappaport, *J. Phys. (Paris) Lett.* **40**, L-219 (1979).

⁷V. K. S. Shante and S. Kirkpatrick, *Adv. Phys.* **20**, 325 (1971); H. Scher and R. Zallen, *J. Chem. Phys.* **53**, 3759 (1970); J. Straley, *Phys. Rev. B* **15**, 5733 (1977).

⁸D. J. Phelps and C. P. Flynn, *Phys. Rev. B* **14**, 5279 (1976), and references therein.

⁹E. Abrahams, P. W. Anderson, D. C. Licciardello, and T. V. Ramakrishnan, *Phys. Rev. Lett.* **42**, 673 (1979).

¹⁰Y. Imry, *Phys. Rev. Lett.* **44**, 469 (1980).

¹¹M. Kaveh and N. F. Mott, *J. Phys. C* **15**, L697 (1982);

N. F. Mott, *Philos. Mag.* **B 44**, 265 (1981).

¹²W. L. McMillan, *Phys. Rev. B* **24**, 2739 (1981).

¹³T. F. Rosenbaum, K. Andres, G. A. Thomas, and R. N. Bhatt, *Phys. Rev. Lett.* **45**, 1723 (1980); M. A. Paalanen, T. F. Rosenbaum, G. A. Thomas, and R. N. Bhatt, *ibid.* **48**, 1284 (1982).

¹⁴K. Epstein, Ph.D. thesis, University of Minnesota, School of Physics and Astronomy, 1982 (unpublished).

¹⁵Yu. F. Komnik, *Fiz. Nizk. Temp.* **8**, 3 (1982) [*Sov. J. Low Temp. Phys.* **8**, 1982], and references therein.

¹⁶W. Visscher and M. Bolsterli, *Nature (London)* **239**, 504 (1972).

¹⁷P. Chaudhari, A. N. Broers, C. C. Chi, R. Laibowitz, E. Spiller, and J. Viggiano, *Phys. Rev. Lett.* **45**, 930 (1980).

¹⁸P. W. Anderson, *J. Phys. Chem. Solids* **11**, 26 (1959).

¹⁹K. Epstein, A. M. Goldman, and A. M. Kadin, *Phys. Rev. Lett.* **47**, 534 (1981); *Physica* **109B**, 2087 (1982); also following paper, *Phys. Rev. B* **27**, 6690 (1983).

²⁰S. Maekawa and H. Fukuyama, *J. Phys. Soc. Jpn.* **51**, 1380 (1981).

²¹Y. Imry and M. Strongin, *Phys. Rev. B* **24**, 6353 (1981).

²²W. McMillan (private communication).